Electronic Supplementary Information

Halogen-Induced Internal Heavy-Atom Effect Shortening Emissive Lifetime and Improving Fluorescence Efficiency of Thermally Activated Delayed Fluorescence Emitter

Yepeng Xiang,[a,†] Yongbiao Zhao,[b,†] Nan Xu,[a] Shaolong Gong,[a] Fan Ni,[a] Kailong Wu,[a] Jiajia Luo,[a] Guohua Xie,[a] Zheng-Hong Lu,*[b] Chuluo Yang*[a]*

Y. Xiang, N. Xu, Prof. S. Gong, F. Ni, K. Wu, J. Luo, Prof. G. Xie and Prof. C. Yang

Hubei Collaborative Innovation Center for Advanced Organic Chemical Materials, Hubei Key Lab on Organic and Polymeric Optoelectronic Materials, Department of Chemistry, Wuhan University, Wuhan 430072, People's Republic of China

*E-mail: slgong@whu.edu.cn, clyang@whu.edu.cn

Dr. Y. Zhao and Prof. Z.-H. Lu

Department of Materials Science and Engineering, University of Toronto, 184 College St., Toronto, Ontario M5S 3E4, Canada

*E-mail: zhenghong.lu@utoronto.ca

[†] These authors contributed equally to this work.

General information

All the reagents and solvents used for the synthesis or measurements were commercially available, and used as received unless otherwise stated. The ^{1}H NMR and ^{13}C NMR spectra were recorded on Bruker Advanced II (400 MHz) spectrometer with $CDCl_3$ as the solvent and tetramethylsilane (TMS) as an internal reference. Elemental analysis of carbon, hydrogen, and nitrogen was performed on a Vario EL III microanalyzer. Molecular masses were determined by a Thermo Trace DSQ II GC/MS. Thermogravimetric analysis (TGA) and differential scanning calorimetry (DSC) were performed on NETZSCH STA 449C instrument and NETZSCH DSC 200 PC unit under a nitrogen atmosphere, respectively. The thermal stability of the samples was determined by measuring their weight loss, heated at a rate of 10 ^{o}C min^{-1} from room temperature to 600 ^{o}C. The glass transition temperature (T_g) was determined from the second heating scan at a heating rate of 10 ^{o}C min^{-1} from -60 to 220 ^{o}C. UV−Vis absorption spectra were recorded on a Shimadzu UV-2501 recording spectrophotometer with baseline correction. Photoluminescence (PL) spectra were recorded on a Hitachi F-4600 fluorescence spectrophotometer. Cyclic voltammetric (CV) studies of the compounds were carried out in nitrogen-purged dichloromethane (CH_2Cl_2) at room temperature with a CHI voltammetric analyzer. n-Bu_4PF_6 (0.1 M) was used as the supporting electrolyte. The conventional three-electrode configuration consists of a platinum working electrode, a platinum wire auxiliary electrode, and an Ag wire pseudo-reference electrode with ferrocene (Fc/Fc^+) as the external standard. The HOMO energy levels (eV) of the compounds were calculated according to the formula: $-[4.8+(E_{1/2(ox/red)}-E_{1/2(Fc/Fc^+)})]$eV. The LUMO energy levels (eV) of the compounds were calculated according to the formula: $-[4.8-(E_{1/2(red/ox)}-E_{1/2(Fc/Fc^+)})]$eV. The PL lifetimes was measured by a single photon counting spectrometer from Edinburgh Instruments (FLS920) with a Picosecond

Pulsed UV-LASTER (LASTER377) as the excitation source. Absolute PLQYs were obtained using a Quantaurus-QY measurement system (C9920-02, Hamamatsu Photonics) and all the samples were excited at 340 nm. Ground state structures and FMOs were obtained by B3LYP density functional method with basis set 6-31G(d). Time-dependent DFT by functionals B3LYP with basis set 6-311+G(d,p) were performed to further analyse the excited states with the optimized ground state structures.

X-Ray Structural Analysis

The single crystal of ClPPM was achieved from solvent diffusion method from dichloromethane /*n*-hexane. Single-crystal X-ray-diffraction data were obtained from a Bruker APEX2 Smart CCD diffractometer through using MoKα radiation (λ = 0.71073 Å) with a $\omega/2\theta$ scan mode at 296 K. Structures of the crystals were solved by direct methods using the APEX2 software. None-hydrogen atoms were refined anisotropically by full-matrix least-squares calculations on F^2 using APEX2, while the hydrogen atoms were directly introduced at calculated position and refined in the riding mode. Drawings were produced using Mercury-3.3. CCDC-1538032 (ClPPM) contains supplementary crystallographic data. These data can be obtained free of charge from the Cambridge Crystallographic Data Centre *via* www.ccdc.cam.ac.uk/data_request/cif.

Device fabrication and measurement

The electron-injection material of LiF was purchased from Sigma-Aldrich and used as received. The hole-transporting materials of tris(4-(9*H*-carbazol-9-yl)phenyl)amine (TCTA) and 4,4'-(cyclohexane-1,1-diyl)bis(*N,N*-di-p-tolylaniline) (TAPC), host material of 4,4'-di(9*H*-carbazol-9-

yl)-1,1'-biphenyl (CBP), and electron transport material of 1,3,5-tri(*m*-pyrid-3-yl-phenyl)benzene (TmPyPB) were purchased from Luminescence Technology Corporation and used as received. Devices were fabricated in a Kurt J. Lesker LUMINOS cluster tool with a base pressure of 10^{-7} Torr without breaking vacuum. The ITO anode was commercially patterned and coated on glass substrates with a thickness of 120 nm and sheet resistance of 15 Ω per square. Prior to loading, the substrate was degreased with standard solvents, blow-dried using a N_2 gun, and treated in a UV−ozone chamber. The active area for all devices was 2 mm^2. Before removing the devices from the vacuum for characterization they were encapsulated by a 500 nm thick layer of SiO_2 deposited by thermal evaporation. Luminance−voltage measurements were carried out using a Minolta LS-110 Luminance Meter. Current−voltage characteristics were measured using an HP4140B pA meter. The electroluminescence spectra were measured using an Ocean Optics USB4000 spectrometer calibrated with a standard halogen lamp. The radiant flux for calculating EQEs was measured using an integrating sphere equipped with an Ocean Optics USB4000 spectrometer with NIST traceable calibration using a halogen lamp.

Synthesis of materials

All reagents were used as received from commercial sources and used as received unless otherwise stated.

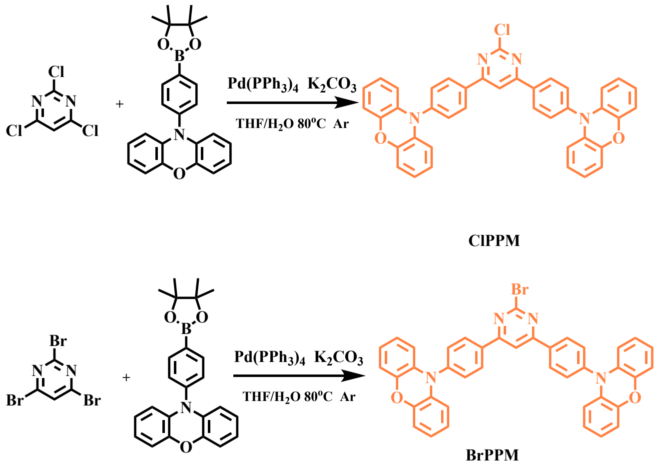

Scheme S1. Synthesis route of ClPPM and BrPPM.

10,10'-((2-Chloropyrimidine-4,6-diyl)bis(4,1-phenylene))bis(10*H*-phenoxazine) (ClPPM): To a mixture of 10-(4-(4,4,5,5-tetramethyl-1,3,2-dioxaborolan-2-yl)phenyl)-10*H*-phenoxazine (847 mg, 2.2 mmol), 2,4,6-trichloropyrimidine (183 mg, 0.12 mL, 1 mmol), potassium carbonate(552 mg, 4 mmol) and $Pd(PPh_3)_4$ (10 mg, 0.01 mmol) was added 20 mL of degassed tetrahydrofuran and 10 mL of degassed water. The suspension was stirred at 80 ^{o}C under a nitrogen atmosphere for 24 h. The mixture was cooled down to room temperature and mixed thoroughly with 3 × 20 mL of dichloromethane. The collected organic phase was washed with water and dried with anhydrous Na_2SO_4. After filteration and removal of the solvent, the residue was purified by column chromatography on silica gel (eluent: petroleum /dichloromethane = 1:1, v/v) to afford the title compound as red powder (453 mg, yield: 72%). ^{1}H NMR (400 MHz, $CDCl_3$ + TMS, 25 ^{o}C) δ [ppm]: δ 8.40 (d, J = 8.6 Hz, 4H), 8.13 (s, 1H), 7.57 (d, J = 8.6 Hz, 4H), 6.74-6.60 (m, 12H), 6.00 (d, J = 9.3 Hz, 4H). ^{13}C NMR (100 MHz, $CDCl_3$, 25 ^{o}C) δ [ppm]: 166.92, 162.40, 143.99, 142.48, 135.59, 133.80, 131.81, 130.30, 123.31, 121.85, 115.70, 113.26, 111.25. MS (EI): *m/z* 628.14 [M^+]. Anal. Calcd for $C_{40}H_{25}ClN_4O_2$: C 76.37, H 4.01, N 8.91. found: C 76.26, H 4.11, N 8.96

10,10'-((2-Bromopyrimidine-4,6-diyl)bis(4,1-phenylene))bis(10*H*-phenoxazine) (BrPPM): The title compound was synthesized according to the similar procedure as ClPPM, but with 2,4,6-tribromopyrimidine (316 mg, 1 mmol) to replace 2,4,6-trichloropyrimidine. Yield: 64%. ^{1}H NMR (400 MHz, $CDCl_3$ + TMS, 25 °C) δ [ppm]: δ 8.39 (d, J = 8.5 Hz, 4H), 8.16 (s, 1H), 7.57 (d, J = 8.5 Hz, 4H), 6.75-6.60 (m, 12H), 6.00 (d, J = 7.8 Hz, 4H). ^{13}C NMR (100 MHz, $CDCl_3$, 25 °C) δ [ppm]: 166.64, 154.20, 143.97, 142.42, 135.50, 133.76, 131.72, 130.29, 123.31, 121.82, 115.72, 113.25, 111.61. MS (EI): *m/z* 671.89 [M^+]. Anal. Calcd for $C_{40}H_{25}BrN_4O_2$: C 71.33, H 3.74, N 8.32. found: C 71.29, H 3.79, N 8.34.

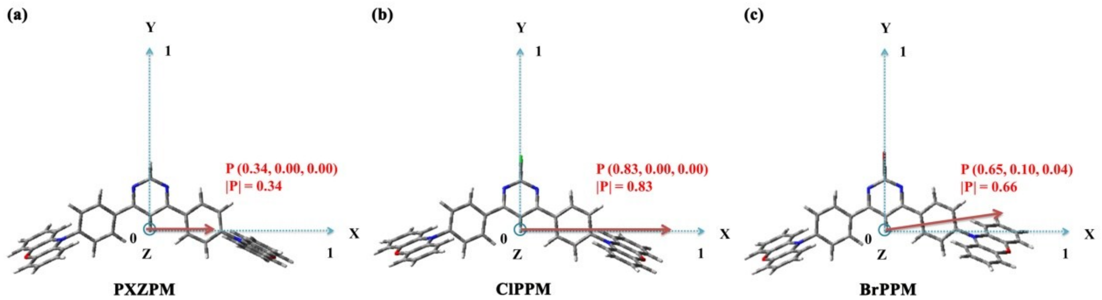

Fig. S1 Optimized molecular structure and transition dipole moments calculated by TD-DFT B3LYP/6-31+G(d,p) for the lowest transition from the ground (S_0) to the excited state (S_1) originating from possible transitions

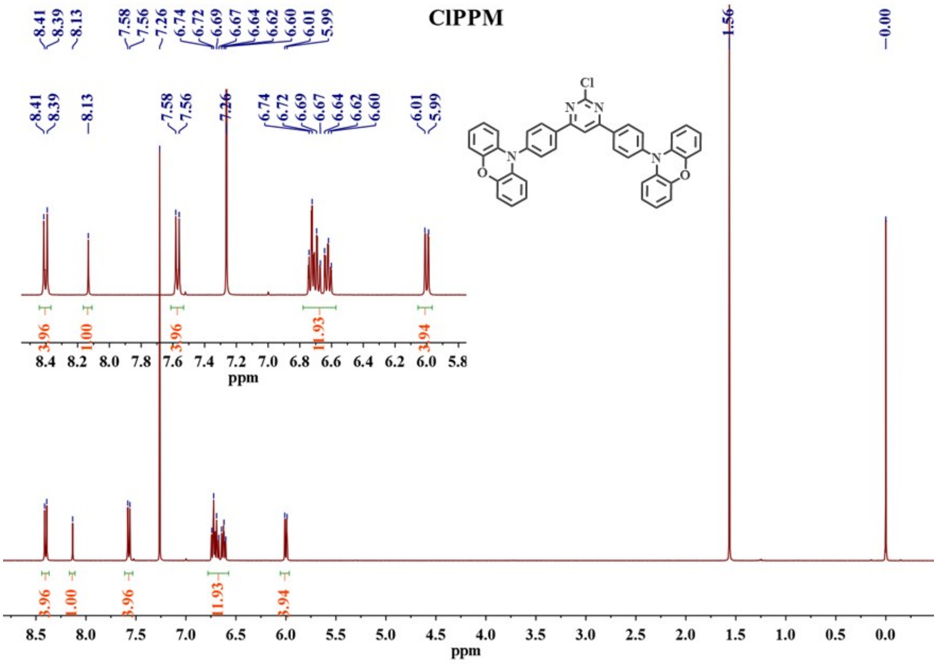

Fig. S2 ^{1}H NMR spectra of ClPPM (400 MHz, $CDCl_3$ + TMS, 25 ^{o}C).

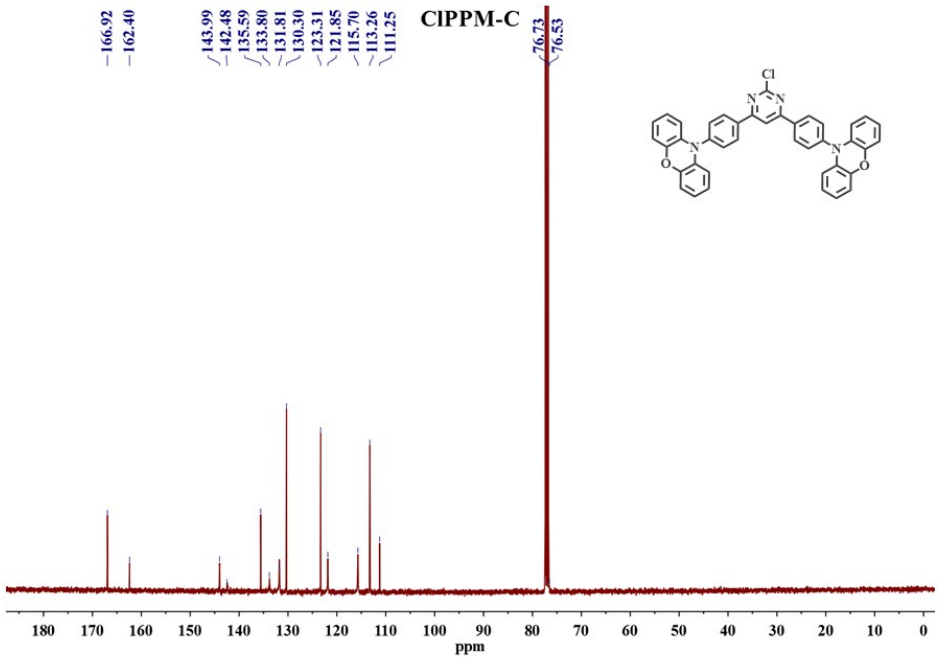

Fig. S3 ^{13}C NMR spectra of ClPPM (100 MHz, $CDCl_3$, 25 ^{o}C).

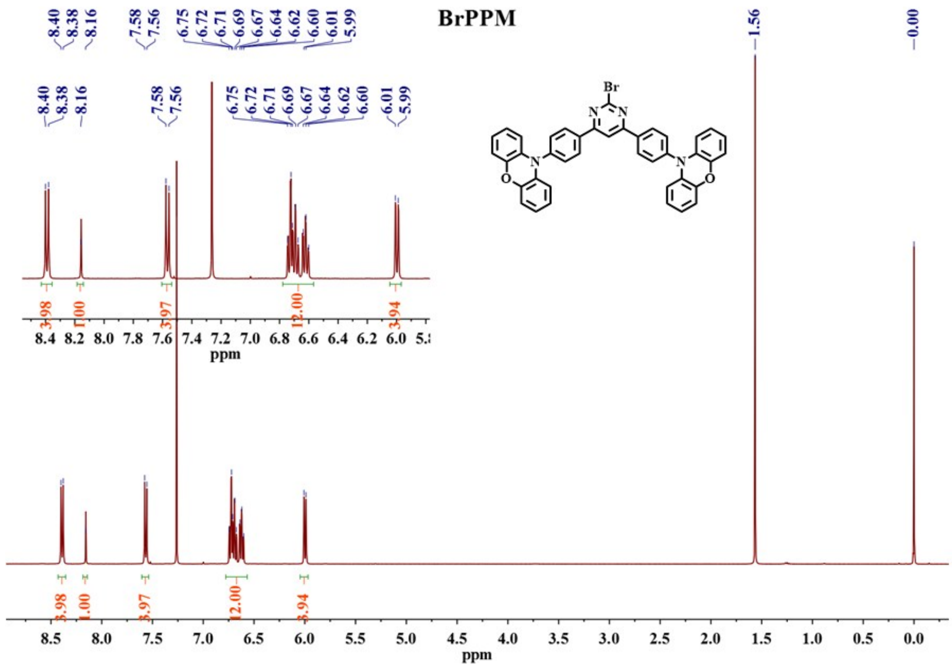

Fig. S4 ^{1}H NMR spectra of BrPPM (400 MHz, $CDCl_3$ + TMS, 25 ^{o}C).

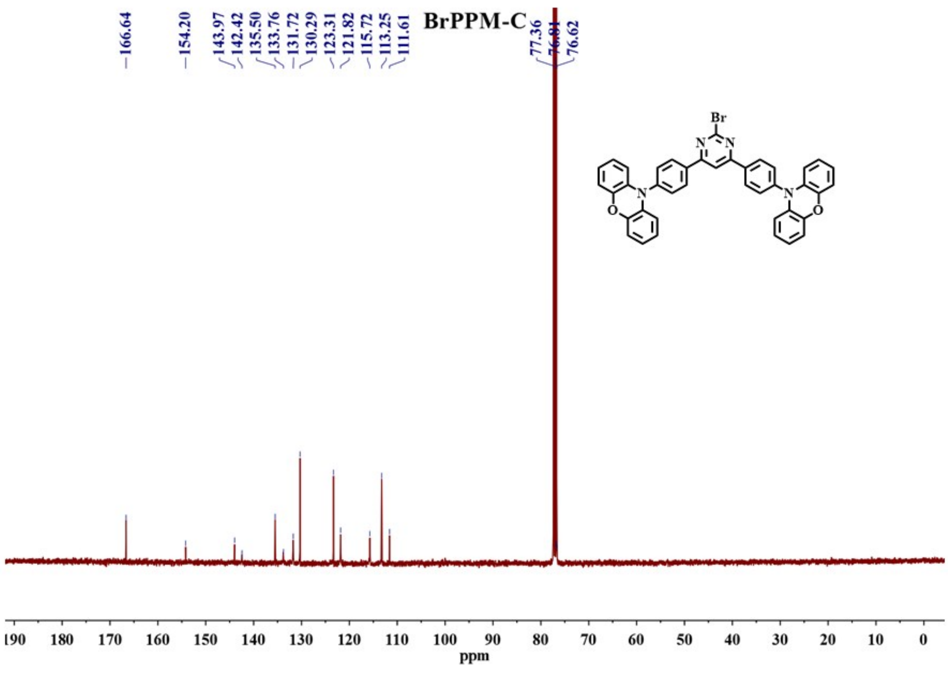

Fig. S5 ^{13}C NMR spectra of BrPPM (100 MHz, $CDCl_3$, 25 ^{o}C).

Table S1. Detail single crystal X-ray diffraction data of ClPPM.

Molecules	ClPPM
CCDC	1538032
Temperature:	296(2) K
Moiety formula:	$2(C_{40}H_{25}ClN_4O_2)$, CH_2Cl_2

Formula weight:	1343.10
Crystal system:	Triclinic
Space group:	P-1
a (Å):	9.0807(7)
b (Å):	12.8892(10)
c (Å):	15.1975(11)
alpha (deg.):	67.580(2)
beta (deg.):	83.551(2)
gamma (deg.):	88.048(2)
Volume(Å^3):	1633.8(2)
Z:	1
Dx (g/cm^3):	1.365
Mu(mm^{-1}):	0.243
F(000):	694
Final R indices [*I*>2_(*I*)]:	R_1 = 0.0756, ωR2 = 0.2298
R indices (all):	R_1 = 0.0964, ωR2 = 0.2584
Goodness-of-fit on F^2:	0.978

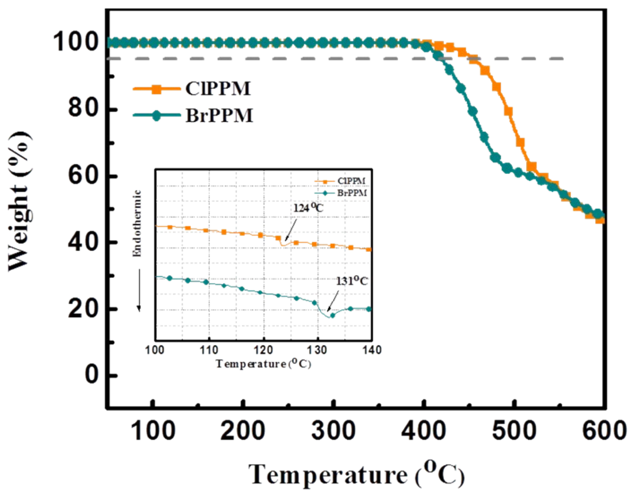

Fig. S6 TGA (Inset: DSC) curves of ClPPM and BrPPM.

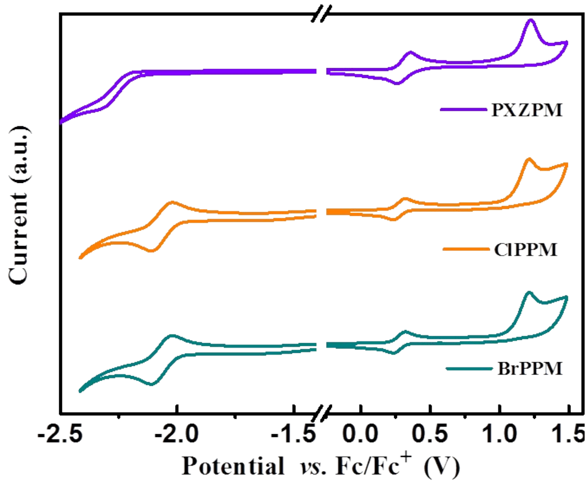

Fig. S7 Oxidation and reduction behaviors of PXZPM, ClPPM and BrPPM.

Table S2. Thermal, electrochemical and TD-DFT calculation data of the compounds

Compound	HOMO/LUMO[a] [eV]	HOMO/LUMO[b] [eV]	f^c	$S_1{}^c$ [eV]	$T_1{}^c$ [eV]	$\Delta E_{ST}{}^c$ [eV]	$T_g{}^d/T_m{}^d/T_d{}^e$[°C]
PXZPM	-5.10/-2.54	-4.74/-2.18	0.0059	2.11	2.09	0.02	115/-/488
ClPPM	-5.08/-2.86	-4.80/-2.41	0.0326	1.95	1.93	0.02	124/294/408
BrPPM	-5.08/-2.73	-4.80/-2.42	0.0205	1.95	1.93	0.02	131/308/408

[a]Obtained from Cyclic voltammograms in CH_2Cl_2 solution. [b]Estimated from DFT calculations. [c]Estimated from TD-DFT simulations. [d]Obtained from DSC measurements. [e]Obtained from TGA measurements (T_d, corresponding to 5% weight loss).

The rate constants of ISC (k_{ISC}), RISC (k_{RISC}) and triplet state non-radiative (k^T_{nr}) of three emitters based on the following equations:

$$k_{ISC} = (1 - \Phi_p) * k_p \qquad (1)$$

$$k_{RISC} = \frac{\Phi_d}{\Phi_p} * \frac{k_p * k_d}{k_{ISC}} \qquad (2)$$

$$k_{nr}^{T} = k_d \frac{\Phi_p + \Phi_d}{\Phi_p} - k_{RISC} \quad (3)$$

Where $k_{PF} = \Phi_P/\tau_p$, $k_p = 1/\tau_p$, $k_d = 1/\tau_d$.

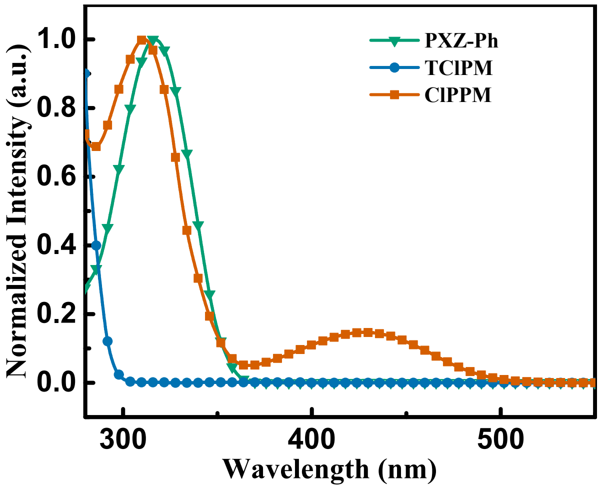

Fig. S8 (a) Normalized UV-Vis absorption spectra of ClPPM, 10-phenyl-10*H*-phenoxazine (Ph-PXZ) and 2,4,6-trichloropyrimidine (TClPM) in toluene solutions (1 x 10^{-5} M) at room temperature.

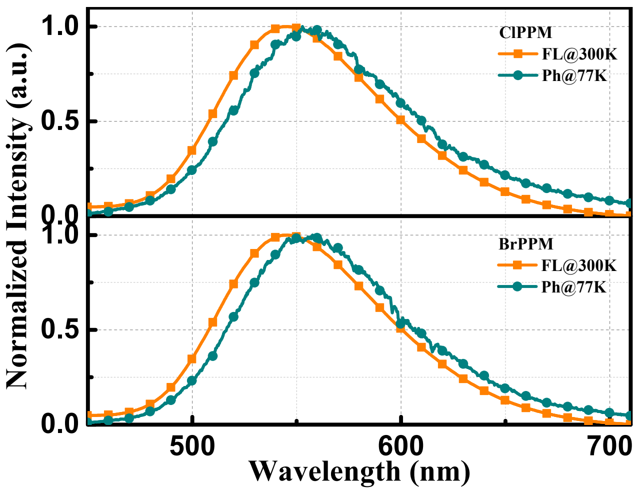

Fig. S9 The fluorescence and phosphorescence spectra of the ClPPM and BrPPM in 1.5 wt.% PMMA doped films.

Table S3. Photophysical data of the two compounds in PMMA doped films

Compounds	λ^{a}_{PL} [nm]	$S_1{}^{b}$ [eV]	$T_1{}^{c}$ [eV]	$\Delta E_{ST}{}^{d}$ [eV]
ClPPM	546	2.58	2.53	0.05
BrPPM	546	2.59	2.52	0.07

[a]Obtained from the peak of the fluorescence spectra in 1.5 wt.% PMMA doped films at room temperature. [b]Calculated from the onset of the fluorescence spectra of two emitters doped into PMMA (1.5 wt.%) at room temperature. [c]Calculated from the onset of the phosphorescence spectra of two emitters doped into PMMA (1.5 wt.%) at room temperature. [d]$\Delta E_{ST} = S_1^b - T_1^c$.

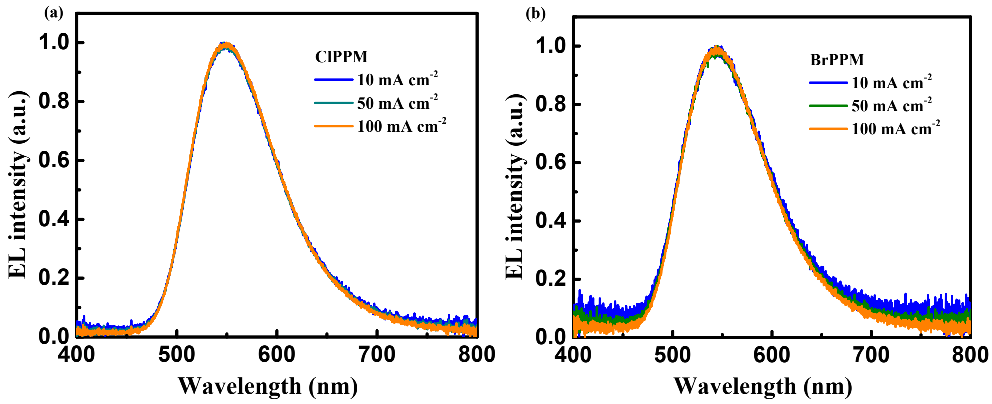

Fig. S10 The EL spectra of devices A-B (1.5 wt.% doped concentration) at various current densities.

Table S4 Electroluminescence characteristics of the devices based on ClPPM

Device	Emitter Doped Concentration [wt.%]	Turn-on Voltage[a] [V]	L_{max}[b] [cd m^{-2}]	Maximum Efficiency[c] CE, PE, EQE	Luminance at 1000 cd m^{-2} CE, PE, EQE	Luminance at 10000 cd m^{-2} CE, PE, EQE	CIE[d](x, y)
A_1	1.5	3.2	32090	68.9, 67.7, 25.3	60.0, 44.5, 22.2	41.3, 20.8, 15.2	(0.40, 0.55)
A_2	3.0	3.1	32010	58.6, 51.2, 22.0	54.2, 40.2, 20.4	36.2, 17.6, 13.6	(0.43, 0.54)
A_3	6.0	3.0	34230	52.0, 45.4, 20.8	49.5, 37.7, 19.8	34.7, 17.0, 13.9	(0.46, 0.52)
A_4	9.0	3.0	35080	45.9, 42.4, 19.0	44.5, 34.2, 18.4	33.0, 16.5, 13.7	(0.47, 0.50)

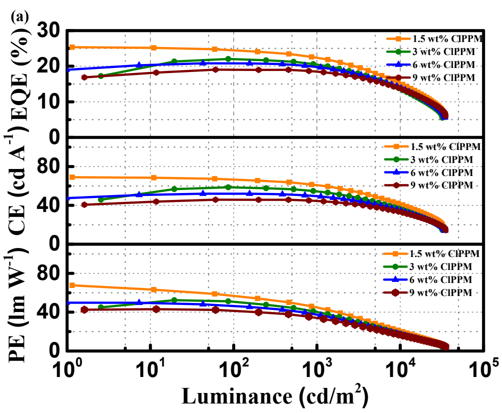

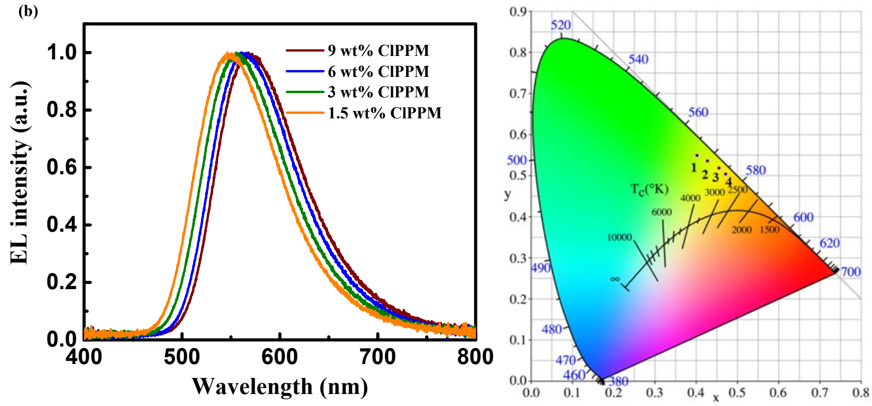

Fig. S11 (a) Power efficiency (PE), current efficiency (CE) and external quantum efficiency (EQE) versus luminance curves of the devices A_1-A_4 based on ClPPM *versus* luminance curves by changing doping concentration for devices with the structure of ITO/TAPC (30 nm)/TCTA (5 nm)/CBP: x wt.% ClPPM (15 nm)/Tm3PyPB (65 nm)/LiF (0.8 nm)/Al (80 nm), where x = 1.5, 3, 6, and 9. (b) Electroluminescence spectra of devices A_1-A_4 at a driving voltage of 8 V and the Commission Internationale de L'Eclairage coordinates recorded at 8 V.

Table S5. Summary performances of green to yellow TADF emitters (500 nm < EL_{max} <580 nm) with high external quantum efficiency (EQE_{max} > 20%)

Compounds	wt.%	EL_{max} [nm]	EQE^{a} (%)			EQE Roll-Off^{b} (%)		Ref.
			Max	@10^3 cd m^{-2}	@10^4 cd m^{-2}	@10^3 cd m^{-2}	@10^4 cd m^{-2}	
BrPPM	1.5	544	23.6	19.8	11.3	16.1	52.1	This work
ClPPM	1.5	547	25.3	22.2	15.2	12.3	39.9	This work
PXZ-MeS_3B	16	502	22.8	~17	-	25.4	-	1
PXZ-PXB	6	503	22.1	~15	~8.5	32.1	61.5	2
TXO-PhCz	5	510	21.5	6	-	72.1	-	3
TmCzTrz	30	500	25.5	~13.5	-	47.1	-	4
DTCBPy	5	514	27.2	14	~6	48.5	77.9	5
DACT-II-9	9	520	29.6	22.8	-	23.0	-	6
DACT-II-19	19	522	27.9	25.3	-	9.3	-	6
Py56	8	550	29.2	20.6	-	29.5	-	7

Pm2	8	526	31.3	13.1	-	58.1	-	7
Pm5	8	541	30.6	20.2	-	34.0	-	7
PXZPM	6	530	19.9	14.2	-	28.6	-	8
PXZPhPM	6	530	24.6	18.2	-	26.0	-	8

[a]The external quantum efficiency. [b]The external quantum efficiency at 1000 cd m^{-2} and at 10000 cd m^{-2} *versus* the maximum external quantum efficiency.

The Equation for the TTA fitting is expressed as:

$$\frac{\eta}{\eta_0} = \frac{J_0}{4J}\left(\sqrt{1 + 8\frac{J}{J_0}} - 1\right) \qquad (4)$$

Where η represents the EQE of the device, η_0 is the device EQE in the absence of TTA, J is the current density of the device, and J_0 is the "onset" current density at $\eta=\eta_0/2$.

Table S6 The EQE_{max} (η_0) and current density (J_0) at half EQE_{max} according to the TTA model

Compounds	EQE_{max} (%)	Roll-off[a] (%)	Roll-off[b] (%)	k_{ISC} [10^7 s^{-1}]	k_{RISC} [10^5 s^{-1}]	J_0 [mA cm^{-2}]
ClPPM	25.3	12.3	39.9	1.90	9.89	48.2
BrPPM	23.6	16.1	52.1	2.05	10.02	26.2
PXZPM	19.9	28.6	69.8	1.19	2.71	13.4

[a]EQE rolling-off at 1000 cd m^{-2}. [b]EQE rolling-off at 10000 cd m^{-2}.

References

1. K. Suzuki, S. Kubo, K. Shizu, T. Fukushima, A. Wakamiya, Y. Murata, C. Adachi and H. Kaji, *Angew. Chem. Int. Ed.*, 2015, **127,** 15446.
2. Y. Kitamoto, T. Namikawa, D. Ikemizu, Y. Miyata, T. Suzuki, H. Kita, T. Sato and S. Oi, *J. Mater. Chem. C*, 2015, **3,** 9122.
3. H. Wang, L. Xie, Q. Peng, L. Meng, Y. Wang, Y. Yi and P. Wang, *Adv. Mater.*, 2014, **26,** 5198.
4. D. R. Lee, M. Kim, S. K. Jeon, S.-H. Hwang, C. W. Lee and J. Y. Lee, *Adv. Mater.*, 2015, **27,** 5861.
5. P. Rajamalli, N. Senthilkumar, P. Gandeepan, P.-Y. Huang, M.-J. Huang, C.-Z. Ren-Wu, C.-Y. Yang, M.-J. Chiu, L.-K. Chu, H.-W. Lin and C.-H. Cheng, *J. Am. Chem. Soc.*, 2016, **138,** 628.
6. H. Kaji, H. Suzuki, T. Fukushima, K. Shizu, K. Suzuki, S. Kubo, T. Komino, H. Oiwa, F.

Suzuki, A. Wakamiya, Y. Murata and C. Adachi, *Nat. Commun.*, 2015, **6,** 8476.
7. K. C. Pan, S. W. Li, Y. Y. Ho, Y. J. Shiu, W. L. Tsai, M. Jiao, W. K. Lee, C. C. Wu, C. L. Chung, T. Chatterjee, Y. S. Li, K. T. Wong, H. C. Hu, C. C. Chen and M. T. Lee, *Adv. Funct. Mater.*, 2016, **26,** 7560.
8. K. Wu, T. Zhang, L. Zhan, C. Zhong, S. Gong, N. Jiang, Z. H. Lu and C. Yang, *Chem. – Eur. J.*, 2016, **22,** 10860.